

Observation of quantum enhanced information erasure

Lorenzo Buffoni¹ and Michele Campisi²

¹*Instituto de Telecomunicações, Physics of Information and Quantum Technologies Group, Lisbon, Portugal*

²*NEST, Istituto Nanoscienze-CNR and Scuola Normale Superiore, I-56127 Pisa, Italy*

Information erasure is one of the basic operations that allow computers, classical and quantum alike, to work. Recent research has elucidated the microscopic mechanisms that are the basis of the physics of information erasure and their energetic cost. Experiments have been carried either in the classical regime (e.g., using optically trapped colloidal particles), or in the quantum regime (e.g., using nanomagnets). Here we employ a quantum annealer to experimentally study the process of information erasure in a macroscopic register whose degree of quantumness can be tuned. This allowed the unprecedented possibility to observe the genuine impact that quantum phenomena have on the physics of information erasure. We report evidence of a triple quantum advantage: the quantum assisted erasure is more effective, faster and more energy efficient. We also observe that the quantum enhancement is so strong that it enables a cooperative erasure of the information individually carried by each qubit forming the register, and that happens with an energy dissipation close to the Landauer bound. We thus demonstrated an effective and energy efficient method to prepare ensembles of qubits in a state of high purity and long time duration, which is a promising tool for quantum computing applications.

Around 20 years ago, Juan Parrondo envisaged a practical realisation of a macroscopic version of Szilard engine that crucially exploits the physics of spontaneous symmetry breaking (SSB) [1]. In the original Szilard design, a single particle is confined in a box, and a separating wall is inserted in the middle of the box, leaving the particle either in the left or right half box with same probability. Knowing where the particle is allows one to extract $kT \log 2$ of energy by isothermally moving the wall in the “right direction” (i.e., that of expansion of the one-particle gas) [2]. Parrondo envisaged an analogous mechanism occurring in a macroscopic system displaying spontaneous symmetry breaking, e.g., a uni-axial Ising ferromagnet. Imagine the magnet is in the paramagnetic state at some temperature T and there is no applied magnetic field B_z , see Fig. 1(a); now increase the spin-spin interaction energy \mathcal{J} , so as to cross its critical value \mathcal{J}_C and so enter the ferromagnetic state. Accordingly, the system collapses onto a state of finite magnetisation, either pointing up or down, with same probabilities [3]; this is analogous to the insertion of the wall of the Szilard engine. Knowing the direction of the magnetisation allows to extract $kT \log 2$ of energy, by circumventing the critical point on the “right side” (i.e., where the applied field points in the same direction as the magnetisation).

Here we note that when run backward, the above protocol implements a spontaneous symmetry breaking induced Landauer’s information erasure [4]. Imagine you start at a point in the ferromagnetic state with no magnetic field, namely with your magnet (your memory) being in the state “up” (the logical 1) or “down” (the logical 0) with same probabilities, see Fig. 1(b). Now you follow Parrondo’s path backward: when you cross the critical value \mathcal{J}_C the system gets very sensitive to the external field, and then by circumventing the critical point from above (below), to return to the ferromagnetic state, the

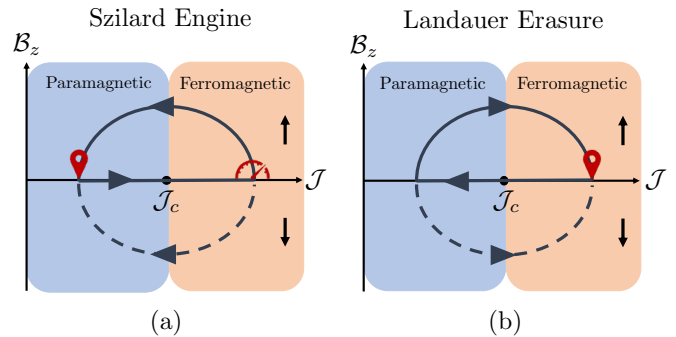


FIG. 1. (a) The Szilard engine protocol described in Ref. [1]. (b) Spontaneous symmetry breaking based Landauer’s erasure protocol implemented in our experiments by using a quantum annealer.

magnet will result in a positive (negative) net magnetisation, regardless of its initial magnetisation. That is, thanks to the peculiar physics of SSB one can map both logical states 0 and 1 onto the single logical state 1 (or 0 depending on the chosen path), which is Landauer’s information erasure.

Despite its fundamental importance, Parrondo’s protocol was never experimentally realised, neither in the original nor in its reversed version. One obvious difficulty is that it requires the manipulation of the spin-spin interaction strength, \mathcal{J} which in a real magnet is a fixed non tunable quantity. Here we overcome this limitation by using a quantum annealer as our experimental platform. This allowed not only to implement, for the first time, the SSB based information erasure illustrated in Fig. 1(b), but also, thanks to the possibility to tune the transverse field, to implement a quantum version thereof and observe the effect of quantum phenomena on the process of memory erasure.

We remark that previous experiments investigating the

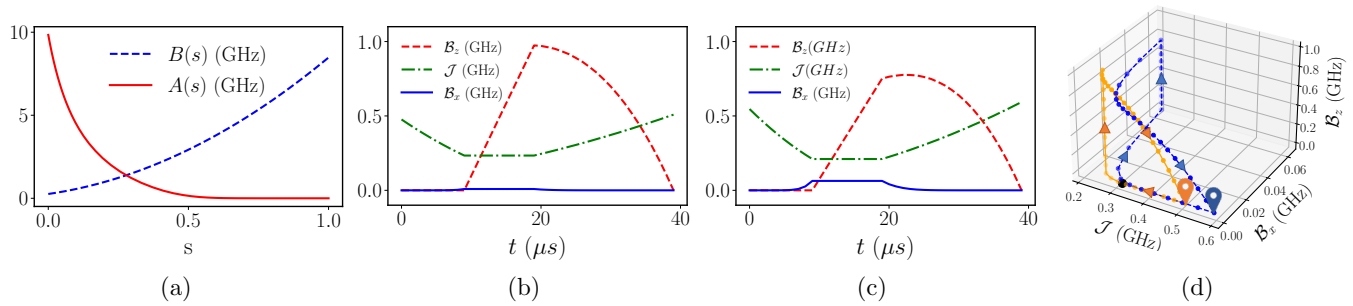


FIG. 2. (a) Control fields $A(s)$ and $B(s)$ of the D-Wave Hamiltonian, Eq.(1), as a function of the schedule parameter s . (b) Driving fields for the classical erasure protocol as a function of time. (c) Driving fields for the quantum erasure protocol as a function of time. (d) Classical (orange solid line) and quantum (blue dashed line) erasure protocols depicted as paths in the space of driving fields. The dots along the paths mark the times $k\delta t$, with $k = 0 \dots 40$, $\delta t = 1\mu s$. The black dot roughly indicates the position of the critical point and pins mark the start and end point of the erasure schedules.

process of information erasure were either conducted in the classical regime [5–10] or in the quantum regime [11], but no experiment so far addressed a hybrid regime where quantum effects were superimposed to classical ones, so as to observe their genuine impact.

Below we report details of our implementation and the experimental results indicating a triple quantum enhancement of information erasure in terms of higher efficacy, faster operation, and lower energetic cost. We also experimentally observe the surprising fact that the quantum enhancement is so strong that it enables a cooperative erasure of the information individually carried by each qubit composing the register, and that happens with an energy dissipation close to the Landauer bound. The method can be applied to prepare collections of qubits in a highly pure and durable quantum state, e.g., for quantum computing applications.

Implementation. – We implemented the SSB based information erasure protocol, Fig. 1(b), on a quantum annealer, specifically the D-Wave Advantage 4.1 processor [12]. It consists of a network of coupled superconducting qubits, whose dynamics is well described by an Ising Hamiltonian in transverse field

$$-\frac{H(s)}{h} = \frac{A(s)}{2} \sum_i \sigma_i^x + \frac{B(s)}{2} \left[g \sum_i \sigma_i^z + \sum_{i,j} J_{ij} \sigma_i^z \sigma_j^z \right] \quad (1)$$

where h is Planck’s constant, σ_i^α denote Pauli operators, and the parameters A and B , with dimensions of frequency, are predetermined functions of the so called annealing parameter s , see Fig. 2(a). The annealing parameter s can be manipulated in time by the user according to some piece-wise linear function of time $s(t)$. This makes the Hamiltonian generally a time-dependent operator. Users have as well some degree of control of the local field g in time. There is also some freedom in choosing the J_{ij} ’s but their value is fixed in time.

In our experiments, the network geometry was that of

a 16×16 square lattice, with constant nearest neighbour interaction $J_{ij} = J$, thus resulting in a Hamiltonian of the form

$$-\frac{H(t)}{h} = \mathcal{B}_x(t) \sum_i \sigma_i^x + \mathcal{B}_z(t) \sum_i \sigma_i^z + \mathcal{J}(t) \sum_{\langle i,j \rangle} \sigma_i^z \sigma_j^z \quad (2)$$

where $\mathcal{B}_x(t) = A(s(t))/2$, $\mathcal{B}_z(t) = B(s(t))g(t)/2$, $\mathcal{J}(t) = B(s(t))J/2$. The choice of bi-dimensional geometry, and relatively large N , was dictated by the necessity of the system to display a classical SSB (there is no SSB in the classical 1D Ising model) [3]. Clearly, the fact that the parameters $\mathcal{B}_x, \mathcal{B}_z, \mathcal{J}$ depend on time through predetermined functions of the annealing parameter, implies that a user does not have full freedom to control them, independently. However, given the hardware constraints, there is enough room to implement a purely classical information erasure protocol (i.e., one with $\mathcal{B}_x(t) \simeq 0$) of the type in Fig. 1(b), and, as well a quantum version thereof featuring non null transverse field $\mathcal{B}_x(t)$.

Figures 2(b) and 2(c) respectively shows the classical and quantum erasure schedules $\mathcal{B}_x(t), \mathcal{B}_z(t), \mathcal{J}(t)$, used in our experiments, which resulted from a careful choice of the functions $s(t)$ and $g(t)$ and the parameter J . Note how in the classical schedule, the quantity \mathcal{B}_x remains approximately null at all times. This was achieved by keeping the annealing parameter s in the region $s \in [0.6, 1]$, where A is approximately null, see Fig. 2(a). In absence of transverse field $\mathcal{B}_x(t)$, all the terms composing the Hamiltonian commute with each other and the dynamics is accordingly classical. For the quantum schedule instead we allowed s to get to lower values and so switch on a non-null \mathcal{B}_x component.

Figure 2(d) shows the classical (orange) and quantum (blue) erasure protocols as closed paths in the $(\mathcal{B}_x, \mathcal{B}_z, \mathcal{J})$ space. Note how the classical protocol is approximately two dimensional (it approximately occurs in the $\mathcal{B}_x = 0$ plane), whereas the quantum path ventures in the $\mathcal{B}_x > 0$ region. Note, in particular, how the classical path,

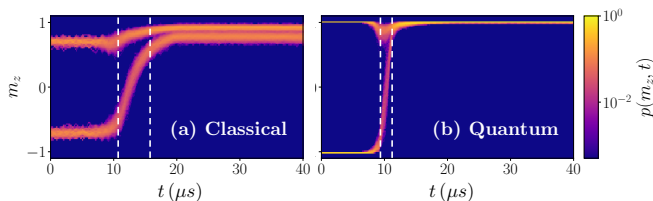


FIG. 3. Experimental probability $p(m_z, t)$ to measure magnetisation density m_z at time t for the classical (a) and quantum (b) erasure protocols.

implements an information erasure protocol of the type depicted in Fig. 1(b). It is worth noticing how in the quantum protocol, the \mathcal{B}_x field is turned on around the crossing of the critical point $\mathcal{B}_x = 0, \mathcal{B}_z = 0, \mathcal{J} = \mathcal{J}_C$, which we roughly estimate to be $\mathcal{J}_C \sim 0.32$ GHz [13].

We initialised the D-Wave Advantage 4.1 [12] quantum annealing processor in a tensor product of eigenvectors of the operators σ_z^i . That is, each qubit was initialised either up or down, according to some statistics (we shall soon comment on the choice of statistics for the classical and quantum cases). We then let evolve the system under the action of the erasure schedule (either the classical or the quantum one) for a time t , and measure the observable σ_z^i for each of the $N = 16 \times 16 = 256$ qubits. This gave us an eigenvalue $s_z^i = \pm 1$ for each qubit, indicating if it is pointing up or down along the z axis. Accordingly, we got a value for the magnetisation density

$$m_z = \sum_i s_z^i / N. \quad (3)$$

This procedure was repeated $\mathcal{N} = 2000$ times. The frequency that a certain value m_z is observed, gives an estimate of the probability $p(m_z, t)$ to find the total system with a magnetisation density m_z at time t . This was done for $t = k\delta$, with $\delta = 1\mu s$, and $k = 1 \dots 40$, to provide a picture of how the probability $p(m_z, t)$ evolves in time for the two protocols. This is depicted in Fig. 3 for both the classical and quantum protocols.

The initial statistics was chosen according to the following criterion: for the classical case we started with a population of all $s_z^i = -1$ and performed the reset protocol which, at the end of the $40\mu s$, converged to a steady state described by some probability distribution $p_1(m_z)$ which statistically describes the logical state 1. The logical state 0 is accordingly described by the distribution, $p_0(m_z) = p_1(-m_z)$. The initial distribution of the classical plot in Fig. 3 is the even combination of logical 0 and logical 1, i.e., $p(m_z, t = 0) = [p_0(m_z) + p_1(m_z)]/2$. For the quantum case, the initial distributions were just chosen to be with all the spin being either $+1$ or -1 with same probability, which approximately conforms to the observed final steady state (almost all spins up). We shall comment on this further below.

Efficacy.— The plots evidence that both methods per-

form very well in terms of the efficacy of the information erasure. We never observed a negative magnetisation density at the end of the protocols, meaning that the probability of such events is smaller the $1/\mathcal{N}$ ($\mathcal{N} = 2000$ is the size of our statistical sample). Indeed we never observed a final net magnetisation density below the value $\langle m_z \rangle = 0.63$ for the classical protocol and $\langle m_z \rangle = 0.98$ for the quantum one.

However, the quality of the distribution that encodes the logical states in the quantum case is extremely higher than that of the classical case. While the magnetization density expectation at the end of the erasure protocol is $\langle m_z \rangle = 0.84 \pm 0.08$ in the classical case, in the quantum case it is $\langle m_z \rangle = 0.998 \pm 0.004$. This means that around 0.2% spins, were not aligned in the positive z direction as a consequence of the quantum assisted information erasure (hence our choice of initial statistics mentioned above).

This evidences a rather unexpected and striking fact, namely that the quantum method not only efficiently erases the information at the macroscopic level, but it efficiently erases the information even at the fine level of each microscopic constituent, i.e., each qubit. This intuition was corroborated by further experiments described below.

Speed.— To assess the speed of the two protocols, we proceeded in the following way. We first introduce a threshold Δ that defines the two logical states of our “magnet”, meaning that a magnetisation density m_z above Δ denotes the logical 1, and a value below $-\Delta$ denotes the logical 0. We chose (with a good degree of arbitrariness) the value $\Delta = 0.5$. Now, considering the switching events only (namely those that began in the logical state 0, i.e., the lower branches in the plots of Fig. 3), we define the switching time as the time that it takes for the average magnetisation m_z to switch from the logical state 0, to the logical state 1. The vertical dashed lines in the Fig. 3 denote the times at which the average m_z crosses the values $\pm\Delta$, and their temporal distance is our measure of the switching time. Despite our limited temporal resolution of $1\mu s$, it is clear that the quantum erasure process is faster than the classical one. The switching time of the quantum protocol is around $2\mu s$ in contrast with the $5\mu s$ required by the classical one.

Energetic cost.— Given a path \mathcal{C} in the space $\mathcal{B}_x, \mathcal{B}_z, \mathcal{J}$ and the according values taken by the their respective conjugated “forces”, namely

$$M_x = \sum_i \langle \sigma_i^x \rangle, M_z = \sum_i \langle \sigma_i^z \rangle, K = \sum_{\langle i,j \rangle} \langle \sigma_i^z \sigma_j^z \rangle \quad (4)$$

where the symbol $\langle \cdot \rangle$ denotes quantum mechanical expect-

tation, the average work cost of the process reads [14]

$$W = - \int_{\mathcal{C}} (M_x d\mathcal{B}_x + M_z d\mathcal{B}_z + K d\mathcal{J}) \doteq W_x + W_z + W_{zz}. \quad (5)$$

As mentioned above, at each point along the path we have collected the eigenvalue of each σ_i^z operator, and repeated the measurement \mathcal{N} times. By averaging over such repetitions gives us an estimate of the expectation values $\langle \sigma_i^z \rangle$ and $\langle \sigma_i^z \sigma_j^z \rangle$. Hence we have a sampling of the forces M_z and K along our paths which can be used to estimate the according works W_z and W_{zz} as discrete sums.

In contrast, we do not have experimental data regarding the expectation values of the σ_x^i operators. However with the available data on $\langle \sigma_i^z \rangle$ we can bound them. Recalling that the quantities $\langle \sigma_i^x \rangle$, $\langle \sigma_i^y \rangle$, $\langle \sigma_i^z \rangle$, are the components of the Bloch vector describing the state of the qubit i , and that said vector has at most length 1, we have

$$|M_x| = \left| \sum_i \langle \sigma_i^x \rangle \right| \leq \sum_i |\langle \sigma_i^x \rangle| \leq \sum_i \sqrt{1 - \langle \sigma_i^z \rangle^2} \doteq M_*$$

where the last term is accessible from our experimental data. Let's break W_x in two contributions, one stemming from the forward branch $\mathcal{B}_x^{\min} \rightarrow \mathcal{B}_x^{\max}$, and one from the backward branch $\mathcal{B}_x^{\max} \rightarrow \mathcal{B}_x^{\min}$ and let $M_x^{F(B)}$, $M_*^{F(B)}$ denote the according average magnetisations and their bounds. We have:

$$\begin{aligned} W_x &= - \int_{\mathcal{B}_x^{\min}}^{\mathcal{B}_x^{\max}} M_x^F d\mathcal{B}_x - \int_{\mathcal{B}_x^{\max}}^{\mathcal{B}_x^{\min}} M_x^B d\mathcal{B}_x \\ &= - \int_{\mathcal{B}_x^{\min}}^{\mathcal{B}_x^{\max}} (M_x^F + M_x^B) d\mathcal{B}_x \leq \int_{\mathcal{B}_x^{\min}}^{\mathcal{B}_x^{\max}} (|M_x^F| + |M_x^B|) d\mathcal{B}_x \\ &= \int_{\mathcal{B}_x^{\min}}^{\mathcal{B}_x^{\max}} (M_*^F + M_*^B) d\mathcal{B}_x \doteq \delta W. \end{aligned}$$

Similarly, $W_x \geq -\delta W$, thus $-\delta W \leq W_x \leq \delta W$.

Then our experimental estimation of the total work W_{exp} reads

$$W_{\text{exp}} = W_z + W_{zz} \pm \delta W \quad (6)$$

where the quantum effects are responsible for the experimental error δW , that needs to be added to the experimental errors on W_z and W_{zz} .

Table I reports the values of W_z , W_{zz} , δW and W_{exp} for the classical and quantum erasure process depicted in Fig. 3 (see 2nd and 3d columns). The most important point to be noted is that the quantum process costs roughly half the work spent by the classical process.

Also note that both processes cost far more than the Landauer cost of one bit erasure $W_L = kT \log 2$.

Quantum cooperative erasure.— To corroborate the intuition that the quantum erasure protocol is so effective

Energy (GHz)	Classical er.	Quantum er.	Qu. coop. er.
W_z	161(12)	50(10)	25(9)
W_{zz}	-53(13)	-1.4(2)	-172(3)
δW	5.5	8	16
U_f			-284.3
W_{exp}	108(30.5)	48.6(20)	137.3(28)
W_L	0.22	0.22	56.3

TABLE I. Experimental values of work contributions for the classical erasure, the quantum erasure (Fig. 3, panels (a) and (b), respectively), and the quantum cooperative erasure (Fig. 4, panel (b)). The uncertainties are reported in parenthesis.

that it actually erases the information at the level of each single qubit, we initialised each qubit of the lattice in a completely random way, (i.e., up or down each with 50% probability), and applied our classical and quantum erasure schedules. The results are depicted in Fig 4. Note how in both cases the whole system is led to a well defined logical state, even if that was not well defined initially.

Most remarkably, in the quantum case, almost every single qubit is taken from its initial random state to the up state. What we are observing is rather surprising: the quantum enhancement is so strong that it enables the joint cooperative erasure of many qubits at the same time, by amplifying the aligning tendency caused by the ferromagnetic interaction. Thus, the results presented in Fig. 4 demonstrate an effective and practical way to turn a maximally mixed ensemble of qubits into one with high degree of purity. Note also that the end state is very stable in the course of time. To further corroborate this fact, we performed further experiments with the final distribution $p(m_z, \tau)$ as initial state and an evolution time of $2000 \mu\text{s}$ (the maximum allowed by the hardware) with the fixed Hamiltonian $H(0)$: no change in the distribution was observed over the course of that time.

Given that our quantum cooperative erasure process efficiently erases the information of N qubits at the same time, a relevant question is how much energy does that costs and, in particular, how does that compare with the Landauer bound. Our initialisation (each qubit is either up or down with same probability) corresponds to the thermal equilibrium of N non interacting qubits in absence of local fields, which are described by the

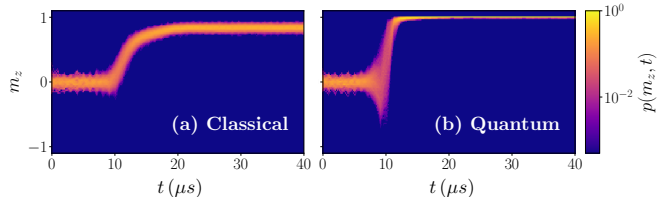


FIG. 4. Experimental probability $p(m_z, t)$ to measure magnetisation density m_z at time t for the classical (a) and quantum (b) protocols and random initialisation of each qubit.

null Hamiltonian $H_0 = 0$. The cooperative erasure process can be seen as implemented through the following sequence: a) the Hamiltonian is quenched from H_0 to $H(0) = -h\mathcal{J}(0)\sum\langle\sigma_i^z\sigma_j^z\rangle$ at $t = 0$ [15]; b) The Hamiltonian evolves in time according to the time dependent schedule $H(t)$ between $t = 0$ and the final time $t = \tau$; c) the Hamiltonian is instantaneously quenched from $H(\tau)$ to H_0 at time $t = \tau$ [16]. Under these conditions, it is known that the cycle is associated in general to a nonnegative work cost $W \geq 0$ (Kelvin formulation of the second law [17]), and if the process successfully realises information erasure of N bits, it must cost at least $W_L = NkT \log 2$ of energy [18, 19].

The total work is the sum of the values of work performed in each stage of the sequence. Regarding the first quench, the energy expectation of the system is null both before and immediately after the quench, hence the change in the system internal energy ΔU is null. Since there is no heat flow to the thermal environment either, $Q = 0$ (because there is no time for that to happen), the work $W = \Delta U - Q$ is also null. Regarding the time interval $(0, \tau)$ the work is given by the line integral in Eq. (5) which can be estimated from the experimental data with some known error, as above. Regarding the second quench, its work cost is given by the change in energy across the quench. Since after the quench it is $H_0 = 0$, the final energy expectation is trivially null, and the negative energy expectation $-U_f = -\langle H(\tau) \rangle_\tau$ over the final state gives the contribution of the quench to the total work. Summing up, the total cooperative work to erase the N bits is

$$W_{\text{exp}} = W_z + W_{zz} - U_f \pm \delta W \quad (7)$$

Table I reports the values of $W_z, W_{zz}, U_f, \delta W, W_{\text{exp}}$ as well as the Landauer bound for the erasure of N bits of information $W_L = NkT \log 2$ (see 4th column). Note how the total work is around twice the Landauer bound, which evidences a very energy efficient process. In this regard it is worth mentioning that the value reported in the table refers to the nominal temperature of 15mK declared by D-Wave. Based on our rough estimation of the critical coupling $\mathcal{J}_C \sim 0.32\text{GHz}$, we deduce that the actual temperature $kT^* = 2\mathcal{J}_C/\log(1 + \sqrt{2})$ is roughly twice the nominal temperature. That means the actual erasure cost was arguably closer to the Landauer bound than the table indicates.

Conclusion.— We have demonstrated an information erasure protocol obtained by inverting Parrondo’s protocol for the Szilard engine [1]. Our implementation using a quantum annealer is unique in that it allows not only to effectively implement the protocol, which is classical, but also to realise a quantum version thereof and so to directly observe the impact of quantum phenomena on the process of information erasure. We observed that the quantum erasure of information carried by a magnetic register is faster, more effective, and requires less

energy consumption, than its classical counterpart. Most remarkably, the quantum erasure protocol is so effective that it erases information at the level of the individual constituents of the register (i.e., individual qubits on the quantum processor) at an energy cost close to Landauer bound. We thus demonstrated an effective and energy efficient method to initialise ensembles of qubits in a quantum state of high purity and long duration, which makes it a promising tool for quantum computing applications.

Acknowledgements.— Access to D-Wave services was provided by CINECA through the competitive ISCRA-C project “q-land”. LB gratefully acknowledges The Blanceflor Foundation for financial support through the project “Large Deviations approach to Landauer’s Principle (LanDev)”. The authors thank Yasser Omar for comments on the manuscript.

-
- [1] Juan M. R. Parrondo. The Szilard engine revisited: Entropy, macroscopic randomness, and symmetry breaking phase transitions. *Chaos*, 11(3):725–733, 2001.
 - [2] Koji Maruyama, Franco Nori, and Vlatko Vedral. Colloquium: The physics of Maxwell’s demon and information. *Rev. Mod. Phys.*, 81:1–23, Jan 2009.
 - [3] N. Goldenfeld. *Lectures On Phase Transitions And The Renormalization Group*. CRC Press, Boca Raton, 1st edition, 1992.
 - [4] R. Landauer. Irreversibility and heat generation in the computing process. *IBM J. Res. Dev.*, 5(3):183–191, 1961.
 - [5] Antoine Berut, Artak Arakelyan, Artyom Petrosyan, Sergio Ciliberto, Raoul Dillenschneider, and Eric Lutz. Experimental verification of Landauer’s principle linking information and thermodynamics. *Nature*, 483(7388):187–189, 2012.
 - [6] Antoine Bérut, Artyom Petrosyan, and Sergio Ciliberto. Information and thermodynamics: experimental verification of Landauer’s erasure principle. *J. Stat. Mech.: Theory Exp.*, 2015:P06015, 2015.
 - [7] Yonggun Jun, Momčilo Gavrilov, and John Bechhoefer. High-precision test of Landauer’s principle in a feedback trap. *Phys. Rev. Lett.*, 113:190601, 2014.
 - [8] Jeongmin Hong, Brian Lambson, Scott Dhuey, and Jeffrey Bokor. Experimental test of Landauer’s principle in single-bit operations on nanomagnetic memory bits. *Sci. Adv.*, 2(3), 2016.
 - [9] Salambô Dago, Jorge Pereda, Nicolas Barros, Sergio Ciliberto, and Ludovic Bellon. Information and thermodynamics: Fast and precise approach to Landauer’s bound in an underdamped micromechanical oscillator. *Phys. Rev. Lett.*, 126:170601, Apr 2021.
 - [10] Gregory Wimsatt, Olli-Pentti Saira, Alexander B. Boyd, Matthew H. Matheny, Siyuan Han, Michael L. Roukes, and James P. Crutchfield. Harnessing fluctuations in thermodynamic computing via time-reversal symmetries. *Phys. Rev. Research*, 3:033115, 2021.
 - [11] R. Gaudenzi, E. Burzurí, S. Maegawa, H. S. J. van der Zant, and F. Luis. Quantum Landauer erasure with a molecular nanomagnet. *Nat. Phys.*, 14(6):565–568, 2018.

- [12] <https://docs.dwavesys.com/docs/latest/index.html>, Visited on 2022.
- [13] To estimate \mathcal{J}_C we made several slow forward annealing ramps and measured the final average magnetization. The ramps were taken as $s(t) = t/\tau$ for $\tau = 200\mu s$. We repeated this process for different values of the coupling J and keeping $g = 0$, then plotted the graph of the magnetization as a function of J . The critical point was then estimated as the point above which we observed a noticeable deviation from zero of the magnetization curve.
- [14] Accordingly, energies will be expressed in Hz. Multiplying them by Planck's constant h gives their value in Joules.
- [15] The fact that this quench was not actually implemented is irrelevant for the subsequent analysis.
- [16] The fact that this quench was not practically implemented is irrelevant as no dynamical evolution is considered thereafter.
- [17] A. E. Allahverdyan and T. M. Nieuwenhuizen. A mathematical theorem as the basis for the second law: Thomson's formulation applied to equilibrium. *Physica A*, 305:542, March 2002.
- [18] Massimiliano Esposito, Katja Lindenberg, and Christian Van den Broeck. Entropy production as correlation between system and reservoir. *New J. Phys.*, 12:013013, 2010.
- [19] Lorenzo Buffoni and Michele Campisi. Spontaneous fluctuation-symmetry breaking and the Landauer principle. *J. Stat. Phys.*, 186(2):31, 2022.